AGU ADVANCING EARTH AND SPACE SCIENCES

Geophysical Research Letters

RESEARCH LETTER
10.1029/2023GL106802

# Magnesium Isotopes Archive the Initial Carbonate Abundances of Metasedimentary Rocks Prior to Thermal Decarbonation

**Qingshang Shi[1], Yongsheng He[1], Zhidan Zhao[1], Franco Rolfo[2], Chiara Groppo[2], Nigel Harris[3], Hongjie Wu[1], Ningyuan Qi[1], and Shan Ke[1]**

[1]State Key Laboratory of Geological Processes and Mineral Resources, Frontiers Science Center for Deep-time Digital Earth, China University of Geosciences, Beijing, China, [2]Department of Earth Sciences, University of Torino, Torino, Italy, [3]School of Environment, Earth and Ecosystem Sciences, Open University, Milton Keynes, UK

**Key Points:**

- A strong correlation between bulk $\delta^{26}$Mg of carbonate-bearing metasedimentary rocks and their initial carbonate abundances was established
- Despite different carbonate species in protoliths, both the calcite-rich and dolomite-rich samples show nearly identical correlations
- Steady state box-model on the carbonate preservation efficiency of continent indicates it is a notable force to regulate atmospheric $CO_2$

**Supporting Information:**

Supporting Information may be found in the online version of this article.

**Correspondence to:**

Y. He and Z. Zhao,
heys@cugb.edu.cn;
zdzhao@cugb.edu.cn

**Citation:**

Shi, Q., He, Y., Zhao, Z., Rolfo, F., Groppo, C., Harris, N., et al. (2024). Magnesium isotopes archive the initial carbonate abundances of metasedimentary rocks prior to thermal decarbonation. *Geophysical Research Letters*, *51*, e2023GL106802. https://doi.org/10.1029/2023GL106802

Received 16 OCT 2023
Accepted 16 JUL 2024

**Abstract** Investigating the carbonate preservation efficiency (CPE) of continental crust is crucial to understand the global carbon cycle, which requires constraints on initial carbonate abundances (ICAs) of crustal rocks. To link Mg isotopes to ICAs, we present elemental and Mg isotopic data for Himalayan carbonate-bearing and carbonate-free metasedimentary rocks. Given no evident melt extraction or external-fluid infiltration, ICAs of these samples can be independently estimated by elemental data. Despite different carbonate species in the protoliths, all the samples show congruent relationship between their $\delta^{26}$Mg and ICAs, owing to the elevated carbonate $\delta^{26}$Mg and Mg/Ca in protoliths of calcite-rich samples resulting from diagenetic processes. When collated with literature data, we suggest the observed correlation here can be applied to most carbonate-bearing (meta-)sedimentary rocks. Based on a steady state box-model, we constrained the modern net carbonate accretion flux ($9.50^{+9.50}_{-5.56}$ Tmol/year) and the average time-integrated CPE (~$80^{+20}_{-43}$%) for continental crust.

**Plain Language Summary** Investigating the fate of carbonate preserved in continental crust is fundamental for understanding its role playing in the global carbon cycle, but is hindered by the lack of knowledge about the initial carbonate abundance of metasedimentary rocks prior to modification (e.g., anatexis). By analyzing Himalayan metasedimentary rocks, here we show a congruent relationship between their $\delta^{26}$Mg and initial carbonate abundances, irrespective of their protolith carbonate species, and suggest it is applicable to most carbonate-bearing (meta-)sedimentary rocks. Based on this relationship, the carbonate preservation in continental crust was simulated using a steady state box-model. The results indicate a very high carbonate accretion influx to the continental crust, seven times higher than the C degassing flux in the mid-ocean ridge. Considering explosive degassing of the accreted carbonates during episodic tectonomagmatic events, the continental crust could have been an important driving force for regulating the atmospheric $CO_2$ during Earth's history.

## 1. Introduction

As an important reservoir, the continental crust contains four orders of magnitude more carbon, mostly as carbonates (~75%–80%; Gao et al., 1998; Hunt, 1972), than the Earth's surface system (i.e., the atmosphere, hydrosphere and biosphere) (DePaolo, 2015). Carbonate-bearing rocks as a major sink of atmospheric carbon dioxide accrete to the continental crust by subduction accretion and collisional amalgamation (Zhu et al., 2021), and tend to decarbonate upon deep burying and heating from underplated magmas that cause metamorphism and crustal anatexis (Groppo et al., 2017, 2022; Mason et al., 2017). Carbon exchange between the continental crust and the surface system plays an important role in regulating the atmospheric $CO_2$ balance and the global climate at a geological time scale (i.e., >million years) (Lee et al., 2019). Therefore, the fate of carbonates during continent formation and evolution, that is, the net preservation efficiency of sedimentary carbonates (CPE = residual carbonate abundance/initial carbonate abundance), is significant to evaluate the role of the continental crust as a source and/or sink in the global carbon cycle.

Pure carbonates have extremely high thermal stability in the continental crust. For example, pure calcite has a solidus of about 1460°C at 1 GPa (Byrnes & Wyllie, 1981). In contrast, thermal decarbonation of carbonate-bearing metasedimentary rocks commonly occurs at lower grades (Groppo et al., 2017; Mason et al., 2017;

Rapa et al., 2017), facilitated by the involvement of silicic constituents (Groppo et al., 2022; Stewart et al., 2019). The key to estimating the CPE of metasedimentary rocks is to obtain their initial carbonate abundances (ICAs; i.e., the carbonate abundances in the protoliths prior to thermal decarbonation), since the residual carbonate abundances can be directly observed. Using elemental data, ICAs of metasedimentary rocks can be estimated based on mass balance provided that the silicate components were constrained (Groppo et al., 2021). While for samples that have experienced crustal anatexis and melt extraction, the resulting elemental differentiation undermines the validity of using elemental contents to reveal the ICAs. Thus, a geochemical proxy that can see through the anatexis processes to trace the ICAs of metasedimentary rocks is required.

Given the distinct Mg isotopic compositions between carbonate and silicate components and the limited isotopic fractionation during partial melting processes (see the review by Teng (2017)), Mg isotopes could be a potential tool to quantitatively trace the ICAs of anatectic rocks. A mineralogical (i.e., carbonate abundance) control on bulk Mg isotopic compositions has been previously reported for carbonate-bearing sediments and (meta-)sedimentary rocks (Hu et al., 2017; Qu et al., 2022; Wang et al., 2015). However, due to the low carbonate abundances in the reported (meta-)sedimentary rocks, a quantitative function remains undefined for lithified rocks, especially considering the potential chemical and isotopic differences between unconsolidated sediments and lithified rocks resulting from diagenesis (Berner, 1980; Fantle et al., 2020). These necessitate further investigations on the relationship between bulk Mg isotopic compositions of carbonate-bearing metasedimentary rocks and their ICAs. In the large and hot Himalayan orogenic belt, metamorphic rocks derived from carbonate-bearing protoliths are widespread (Groppo et al., 2021; Rolfo et al., 2017). These lithologies (referred to below as "carbonate-bearing metasedimentary rocks," although some are totally decarbonated) were derived from protoliths consisting of Proterozoic sediments with varying carbonate contents deposited on the northern Indian passive continental margin, and metamorphosed in an internally buffered system (Groppo et al., 2017, 2021; Rapa et al., 2017), making them appropriate targets to investigate this correlation (Text S1 in Supporting Information S1).

Here we report elemental and Mg isotopic data of 9 Himalayan carbonate-free metasedimentary rocks and 23 Himalayan carbonate-bearing metasedimentary rocks which were collected from Bhutan and Nepal Himalaya (Groppo et al., 2021; Rolfo et al., 2017; Shi et al., 2021; Table S1 in Supporting Information S1), to establish the correlation between bulk Mg isotopic compositions and ICAs. In order to reveal the elemental and isotopic characteristics of the present carbonates and silicate components in the carbonate-bearing rocks, five samples were selected to conduct leaching experiments.

## 2. Results

Himalayan carbonate-free metasedimentary rocks have low LOI (0.90–2.38 wt.%), CaO (0.32–1.47 wt.%), MgO (0.67–1.80 wt.%) and high $SiO_2$ (63.13–73.94 wt.%) contents, and relatively homogeneous $\delta^{26}Mg$ ($-0.09 \pm 0.18‰$, 2SD, $N = 8$). By contrast, Himalayan carbonate-bearing metasedimentary rocks show large variations in LOI (0.66–37.56 wt.%), CaO (0.60–42.86 wt.%), MgO (1.97–17.92 wt.%) and $SiO_2$ (11.13–67.34 wt.%) as well as $\delta^{26}Mg$ ($-2.00$–$0.19‰$); $\delta^{26}Mg$ decreases with increasing LOI, CaO, and MgO (Tables S2 and S3 in Supporting Information S1), reflecting their diverse carbonate abundances. Leaching experiments show that the silicate residues from carbonate-bearing samples have lighter $\delta^{26}Mg$ ($-0.48‰$ to $-1.91‰$) than the carbonate-free metasedimentary rocks (Table S4 in Supporting Information S1), indicating the internal isotopic exchange between carbonate and silicate components during prograde metamorphism (Text S3 in Supporting Information S1). Thus, the present carbonate components of carbonate-bearing metasedimentary rocks have not preserved their initial isotopic characteristics.

## 3. Discussion

### 3.1. Initial Carbonate Abundance in Himalayan Metasedimentary Rocks

Himalayan metasedimentary rocks have experienced decarbonation to variable extents, indicated by the formation of Ca-rich minerals (e.g., clinopyroxene) at the expense of carbonate decomposition (Groppo et al., 2017, 2021, 2022) and decoupling of CaO, MgO, and LOI (Table S3 in Supporting Information S1). To reduce the influence of metamorphic decarbonation on the bulk chemical compositions, here we normalize the major elemental contents on a volatile-free bias (i.e., $(Oxide)_N = \frac{Oxide}{Total\text{-}LOI} \times 100$ wt.%). Two distinct compositional trends were identified based on correlations among $(SiO_2)_N$, $(MgO)_N$, and $(CaO)_N$ (Figures 1a–1c). These trends

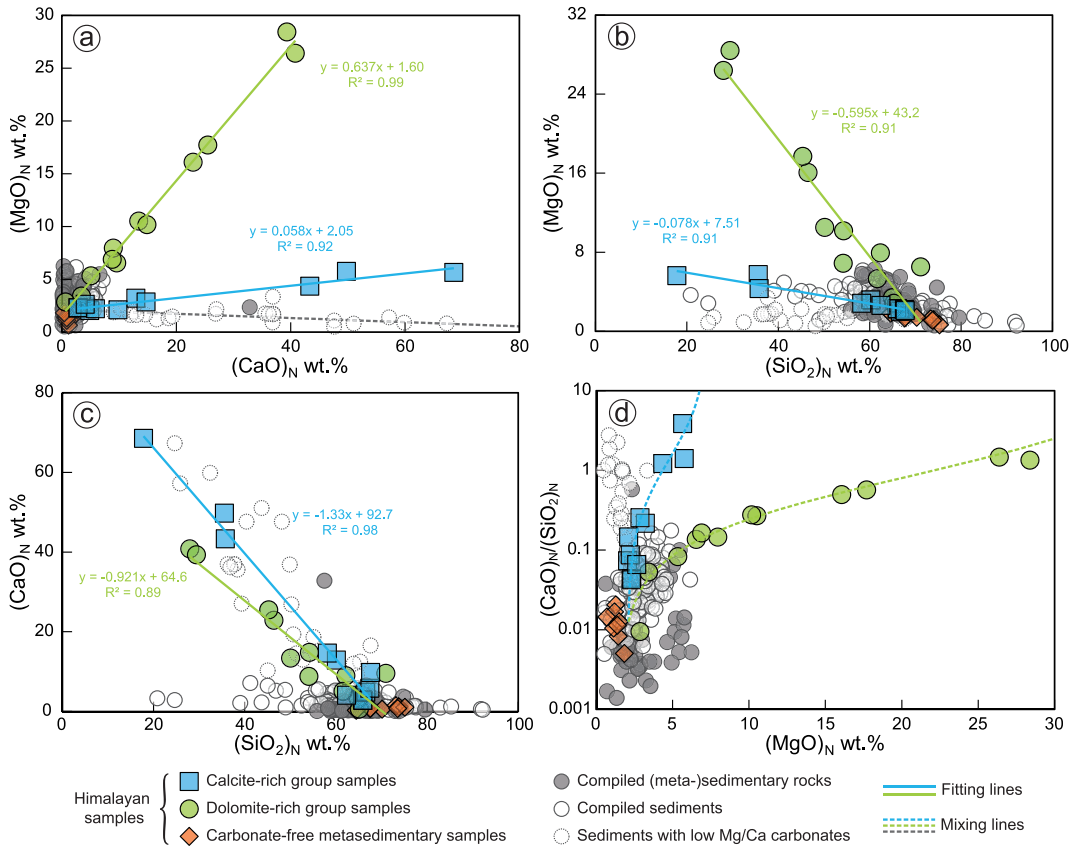


**Figure 1.** Regression analysis on the $(CaO)_N$, $(MgO)_N$, and $(SiO_2)_N$ contents of Himalayan carbonate-bearing metasedimentary rocks (a–c) to obtain the mixing endmember compositions. The gray dashed line denotes mixing between silicate and low-Mg calcite with Mg/Ca = 0.002. (d) Mixing diagram for $(MgO)_N$ and $(CaO)_N/(SiO_2)_N$ ratio with the endmembers constrained by correlations in (a)–(c). The data sources of compiled (meta-)sedimentary rocks and sediments are listed in Table S6 of the Supporting Information S1.

converge at silicate components represented by Himalayan carbonate-free metasedimentary rocks and diverge toward formula dolomite and calcite respectively, consistent with mixing between carbonate and clastic silicate components. Preservation of these compositional trends supports the previous consensus that Himalayan metasedimentary rocks were internally buffered during prograde metamorphism (Groppo et al., 2017, 2021; Rapa et al., 2017). According to the diverse compositional trends, Himalayan carbonate-bearing metasedimentary samples can be divided into two groups, that is, calcite-rich and dolomite-rich samples respectively.

Well-preserved compositional mixing trends between carbonate and clastic silicate components allow us to infer the initial carbonate abundances (ICAs) in Himalayan carbonate-bearing metasedimentary rocks. Regressions between $(CaO)_N$, $(MgO)_N$, and $(SiO_2)_N$ (Figures 1a–1c) indicate consistent compositional endmembers, that is, $Ca_{0.90}Mg_{0.10}CO_3$, $Ca_{0.52}Mg_{0.48}CO_3$ and the silicate endmember that has $(CaO)_N$ (0.79 wt.% in Figure 1a and 0.93 wt.% in Figure 1c; mean = 0.86 wt.%), $(MgO)_N$ (2.10 wt.%) and $(SiO_2)_N$ (69.10 wt.% in Figure 1b and 69.18 wt.% in Figure 1c; mean = 69.13 wt.%) similar to the measured carbonate-free metasedimentary rocks. Based on $(CaO)_N$, $(MgO)_N$, $(CaO)_N + (MgO)_N$, and $(CaO)_N/(SiO_2)_N$, ICAs of carbonate-bearing metasedimentary samples were independently calculated through binary mixing (Table S5 in Supporting Information S1). Note that $(MgO)_N$ is not applicable to quantify ICAs of calcite-rich samples, since the calcite and silicate endmembers show a small MgO difference (4.09 wt.% vs. 2.10 wt.%). Results from different indexes display good consistency, and the ICAs of Himalayan carbonate-bearing metasedimentary rocks are highly variable, ranging from 0.81 wt.% to 83.57 wt.% (Figure S2 in Supporting Information S1). We also calculate the ICA of each sample following the method used by Groppo et al. (2021), which is in good agreement with the result from this study (Table S5 in Supporting Information S1).

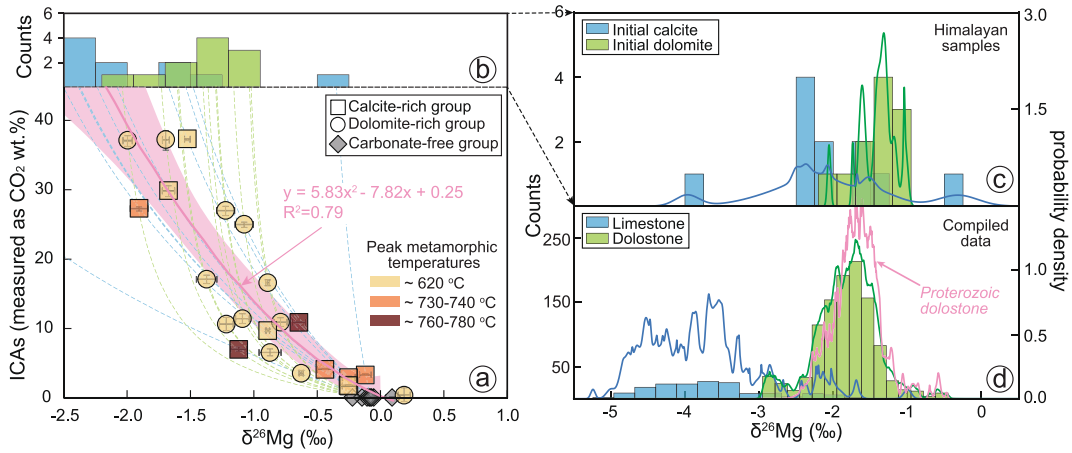


**Figure 2.** (a) The correlation between the ICAs and bulk $\delta^{26}$Mg values for Himalayan carbonate-bearing metasedimentary samples. The regression trend (pink line) and its 95% confidence intervals (pink shaded area) were calculated by a bootstrap resampling method considering both the errors of bulk $\delta^{26}$Mg and ICAs and the scattering of data set (Text S5 in Supporting Information S1). (b, c) The $\delta^{26}$Mg of initial calcites and dolomites from calcite-rich and dolomite-rich metasedimentary samples respectively (Table S5 in Supporting Information S1), which were calculated through binary mixing as indicated by the blue and green dashed lines in (a). Given the low carbonate abundance in sample 17b-15 (−0.81–3.73 wt.%; mean = 0.81 wt.%), its calculated $\delta^{26}$Mg shows a large uncertainty, and thus was not considered. (d) The $\delta^{26}$Mg of compiled global limestones and dolostones, whose data sources were listed in Table S6 of the Supporting Information S1. The lines in (c) and (d) are Kernel density curves with considering the errors of $\delta^{26}$Mg for carbonates.

### 3.2. Mg Isotopic Compositions of Himalayan Metasedimentary Rocks Co-Vary With Their Initial Carbonate Abundances

As ICAs increase, the Himalayan metasedimentary samples show lighter Mg isotopic compositions (Figure 2a). This is consistent with previous observations that the carbonates have relatively lighter Mg isotopic compositions, while the silicate constituents composed of weathered products are enriched in heavy Mg isotopes (Teng, 2017 and references therein). Intriguingly, both the calcite-rich and dolomite-rich samples show roughly identical $\delta^{26}$Mg values at a given ICA despite their different initial carbonate species (Figure 2a). Fitted by quadratic polynomial function using a bootstrap resampling method (details see the Text S5 in Supporting Information S1), the ICA (expressed as $CO_2$ contents; wt.%) equals to $5.83 \times (\delta^{26}\text{Mg})^2 - 7.82 \times \delta^{26}\text{Mg} + 0.25$ ($R^2 = 0.79$). The similar correlations observed in Figure 2a for both group samples are at odds with the expectation from reported distinct Mg isotopic compositions between limestone (mode: −3.69‰) and dolostone (mode: −1.78‰) (Figure 2d). Given that leaching experiments indicate internal isotopic exchange between carbonate and silicate components of Himalayan samples during prograde metamorphism, it is necessary to assess the influence from metamorphic exchange of bulk carbonate-bearing rocks with their wall-rocks (Wang et al., 2014), especially considering most of carbonate-bearing rocks occur as intercalations in the carbonate-free metasedimentary rocks (Rolfo et al., 2017). Two lines of evidence suggest metamorphic exchange with the surrounding carbonate-free rocks is limited. First, Mg isotopic exchange is temperature dependent; higher metamorphic temperatures (i.e., higher metamorphic grades) will lead to smaller Mg isotope fractionations between the carbonate-bearing metasedimentary samples and carbonate-free wall-rocks. Thus, carbonate-bearing metasedimentary samples at higher metamorphic grades would have heavier $\delta^{26}$Mg values if isotopic exchange with carbonate-free wall-rocks occurred. However, the $\delta^{26}$Mg of carbonate-bearing metasedimentary samples do not show any relationship with their metamorphic grades at similar carbonate abundances (Figure 2a). Second, leaching experiments showed that the Mg/Ca of present carbonates from calcite-rich group samples significantly decreased from 0.10 to 0.005 along with increasing metamorphic grades (from ~620°C to ~730–740°C) during the internal metamorphic exchange (Tables S1 and S4 in Supporting Information S1). Similarly, if the carbonate-bearing metasedimentary rocks experienced metamorphic exchange with carbonate-free wall-rocks, MgO will migrate from the carbonate-bearing rocks into the carbonate-free rocks, and the higher the metamorphic grade, the greater the transfer of Mg. The good mixing trend as shown in Figure 1a (i.e., $(MgO)_N$ versus $(CaO)_N$), thus suggests the investigated carbonate-bearing metasedimentary samples maintain their protolith compositions. Accordingly, during prograde metamorphism the elemental and isotopic compositions of carbonate-bearing metasedimentary samples were

only internally redistributed, but did not drive significant metamorphic exchange with surrounding carbonate-free rocks. The $\delta^{26}$Mg values of Himalayan carbonate-bearing metasedimentary rocks therefore reflect the isotopic characteristics prior to prograde metamorphism.

Based on the endmember compositions and initial carbonate abundances estimated above, $\delta^{26}$Mg and its uncertainty of the initial carbonate in each carbonate-bearing metasedimentary sample were calculated from binary mixing (Table S5 in Supporting Information S1), by assuming the silicate endmember having $\delta^{26}$Mg of $-0.09 \pm 0.06$‰ (the average of carbonate-free metasedimentary rocks; Table S2 in Supporting Information S1). The initial dolomites in the dolomite-rich group samples show subtle difference from the compiled dolostone, with relatively heavier $\delta^{26}$Mg (Figures 2c and 2d). Whereas, the initial calcites in the calcite-rich group samples have significantly heavier Mg isotopic compositions than the compiled pure limestone (Figures 2c and 2d). Together with the high Mg/Ca (~0.11) of these initial calcites (vs. <0.01 of pure limestones), the calcite-rich group samples were likely significantly reshaped by diagenetic fluids with high Mg/Ca and heavy $\delta^{26}$Mg (Chanda & Fantle, 2017; Geske et al., 2015; Higgins et al., 2018), which is similar to a partial dolomitization process. Given the large Mg content difference between calcite and dolomite, mild dolomitization can substantially elevate the whole rock Mg isotopic composition toward that of the dolomites, as observed in global carbonates (Figure S5 in Supporting Information S1). Accordingly, we propose that the observed correlation between the $\delta^{26}$Mg and ICAs of Himalayan carbonate-bearing metasedimentary rocks may result from mixing between the clastic silicates and the carbonates which show similar Mg isotopic compositions despite their species due to diagenetic alteration. Further numerical simulation on the diagenesis process for the protoliths of Himalayan carbonate-bearing metasedimentary rocks, which lies out of the scope of this study, could be helpful to elucidate the detailed mechanism.

### 3.3. Implications for Quantifying ICAs of Carbonate-Bearing Samples

The quantitative equation found in this study provides a new geochemical method to quantitatively trace the ICAs of carbonate-bearing samples using Mg isotopes. While considering the reshaping effect from diagenetic processes as revealed by this study, carbonate-bearing samples with diverse degrees of diagenesis shall display varied correlations between their ICAs and $\delta^{26}$Mg. Here, we compare investigated Himalayan samples with the reported Mg isotopic data of global sediments and (meta-)sedimentary rocks to investigate the global applicability of the quantitative equation constrained by Himalayan samples. Benefiting from Himalayan samples extending the range of ICAs for (meta-)sedimentary rocks, these totally lithified samples which have experienced strong diagenesis, show consistent correlations between their $\delta^{26}$Mg and carbonate abundance indexes (e.g., $(CaO)_N + (MgO)_N$ and $(CaO)_N/(SiO_2)_N$). Whereas for the unlithified sediments, some samples with incorporated carbonates that still preserve low Mg/Ca ratios (Figure 1a), indicative of weak diagenetic influence, significantly deviate from the correlations defined by lithified rocks and approach the mixing trends between the silicate endmember and pelagic calcite sediment (Figure 3). These observations suggest that the quantitative equation constrained by Himalayan samples represents a strong diagenesis scenario, and in such circumstances can trace the ICAs of lithified carbonate-bearing samples, including both sedimentary and metasedimentary rocks. For the carbonate-bearing sediments with weak diagenesis, this quantitative equation provides a lower limit of the ICA. Additionally, given this quantitative equation was established on the basis of the samples with ICAs from ~0 to ~83 wt.%, it must be extrapolated with caution to the samples with ICAs that lie out of this range.

Quantifying the ICA is an important prerequisite for investigating the CPE of continental crust. Recently, the identification of $CO_2$-rich fluid inclusions in the granulites and of the nano-carbonatites coexisting with nano-granites from migmatites suggests the decarbonation of carbonate-bearing metasedimentary rocks during anatexis (Ferrero et al., 2016; Tacchetto et al., 2019). However, the chemical differentiation caused by melt extraction during anatexis hampers the use of elemental data to trace the ICAs of the residual metasedimentary rocks. Although the ICA values calculated through Mg isotopes show poor accuracy relative to the elemental estimation method (Figure S3 in Supporting Information S1), the correlation constrained in this study provides a feasible tool for tracing the ICAs of the metasedimentary samples which have experienced anatexis and melt extraction. Moreover, given the limited fractionation during granitic magmatism (Li et al., 2010; Liu et al., 2010), this correlation can also be utilized to trace ICAs in the crustal sources of granites.

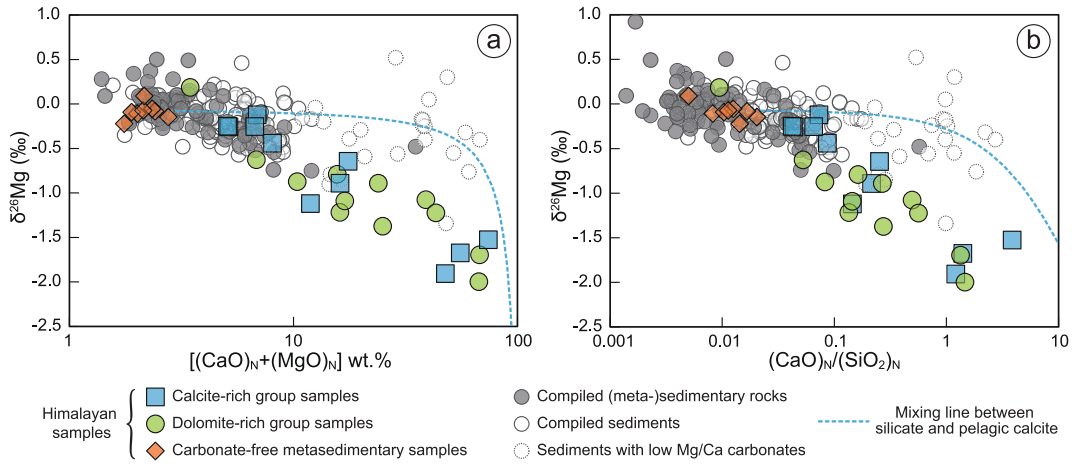


**Figure 3.** $\delta^{26}Mg$ values versus $[(CaO)_N + (MgO)_N]$ (a) and $(CaO)_N/(SiO_2)_N$ values (b) of Himalayan samples, compared with the compiled sediments and (meta-)sedimentary rocks whose data sources were listed in Table S6 of the Supporting Information S1. Dashed line indicates mixing between the silicate endmember and pelagic calcite sediment ($\delta^{26}Mg$: −4.72‰; Mg/Ca = 0.002; Table S6 in Supporting Information S1).

### 3.4. Constraints on the Carbonate Preservation Efficiency (CPE) of Continental Crust

Application of the identified correlation in this study to directly estimate the CPE of crustal rocks is hampered due to the shortage of independent Mg isotopic data for carbonate-bearing metasedimentary rocks from high-grade metamorphic terranes. Here, we establish a steady state box-model on the Mg isotope budget of continental crust (CC) to give a first-order constraint on CPE (Equation 1), considering the Mg outflux by riverine runoff ($J^{Mg}_{runoff}$) and crust destruction ($J^{Mg}_{DO}$) and the Mg influx via mantle-derived magmatic ingrowth ($J^{Mg}_{MI}$) and accretion of continental margin carbonate-bearing sedimentary rocks ($J^{Mg}_{CI}$).

$$\frac{d\delta^{26}Mg_{CC}}{dt} = \frac{J^{Mg}_{MI}\times(\delta^{26}Mg_{MI}-\delta^{26}Mg_{CC})+J^{Mg}_{CI}\times(\delta^{26}Mg_{CI}-\delta^{26}Mg_{CC})-J^{Mg}_{DO}\times(\delta^{26}Mg_{DO}-\delta^{26}Mg_{CC})-J^{Mg}_{runoff}\times(\delta^{26}Mg_{runoff}-\delta^{26}Mg_{CC})}{[Mg]_{CC}} \quad (1)$$

$[Mg]_{CC}$ and $\delta^{26}Mg_{CC}$ represent the Mg content and Mg isotopic composition of the continental crust. Since global granitoids show nearly constant weighted-average $\delta^{26}Mg$ in the past 3.3 billion years, very similar to the mean $\delta^{26}Mg$ of modern continental crust (−0.24 ± 0.07‰; Figure 4a; Yang et al., 2016), the Mg isotope budget of continental crust seems to be in steady state (i.e., $d\delta^{26}Mg_{CC} = 0$). Given the ingrowth magma from deep mantle and destructed crust have similar $\delta^{26}Mg$ to the continental crust (Text S4 in Supporting Information S1), the isotope contribution from Mg input of continental margin sedimentary rock accretion shall thus be in balance with that from Mg output of riverine runoff (Figures 4b and 4c). Accordingly, we can obtain:

$$J^{Mg}_{CI} = \frac{J^{Mg}_{runoff}\times(\delta^{26}Mg_{runoff}-\delta^{26}Mg_{CC})}{\delta^{26}Mg_{CI}-\delta^{26}Mg_{CC}} \quad (2)$$

Based on the average $CO_2$ contents ($[CO_2]_{CI}$; 7.21 wt.%) of continental margin sedimentary rocks (Ronov et al., 1991), its average $\delta^{26}Mg_{CI}$ can be calculated by the correlation constrained in this study (i.e., −0.67 ± 0.13‰, errors in 2 sigma if not specified below; Figure S4 in Supporting Information S1). Other parameters adopted in this study are compiled in Table S7 of the Supporting Information S1. The estimated $J_{CI}$ can be transferred to the carbonate accretion flux ($J_{CO_2\text{-accretion}}$) by the following equation:

$$J_{CO_2\text{-accretion}} = \frac{J^{Mg}_{CI}\times[CO_2]_{CI}}{[MgO]_{CI}} \quad (3)$$

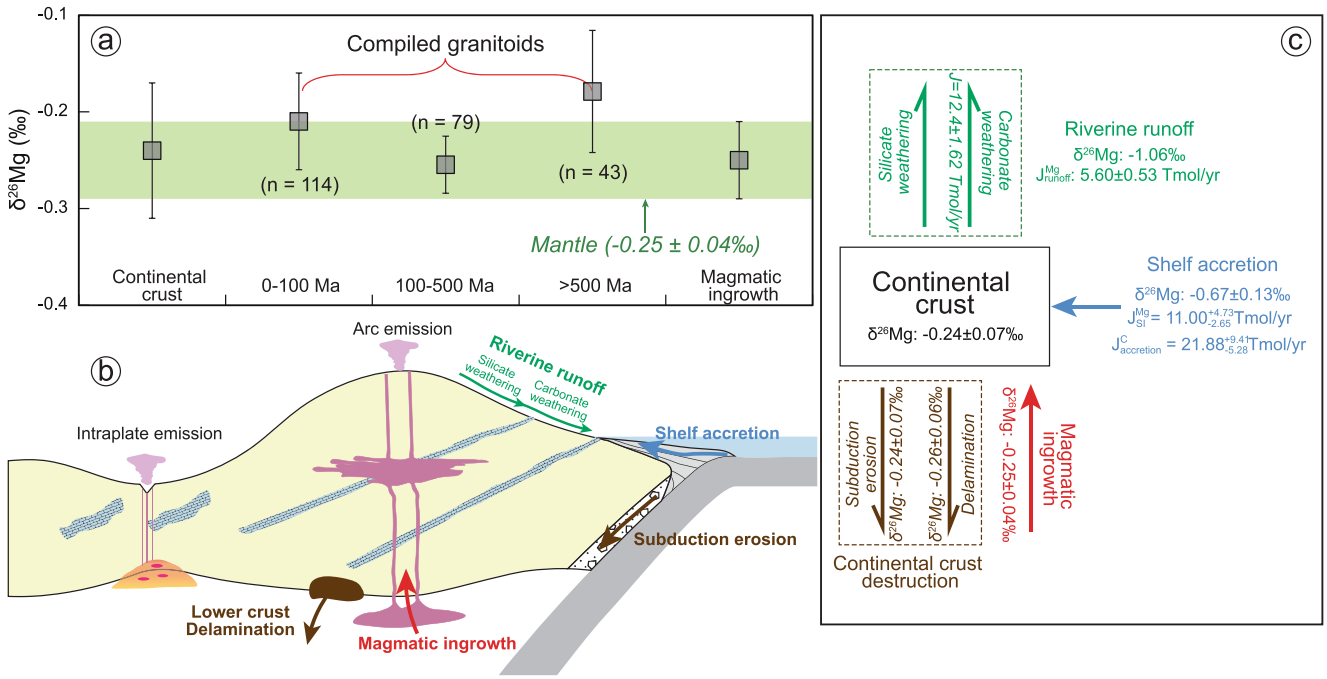


**Figure 4.** (a) The concentration-weighted $\delta^{26}$Mg for compiled granitoids at different time ranges, and comparison with the mantle and continental crust. The data sources are listed in Table S7 of the Supporting Information S1. Cartoon (b) and schematic diagram (c) for the steady state box-model established in this study. The adopted parameters were compiled in Table S7 of the Supporting Information S1.

where $[MgO]_{CI}$ represents the average MgO contents of continental margin sedimentary rocks (3.32 wt.%; Ronov et al., 1991). Part of the accreted carbonates will be returned to the ocean by surficial carbonate weathering (12.4 ± 1.62 Tmol/year; Table S7 in Supporting Information S1). After deducting this carbonate weathering flux, our model indicates a modern net carbonate accretion flux of $9.50^{+9.50}_{-5.56}$ Tmol/year, seven times higher than the *C* degassing flux from the mid-ocean ridge (1.34 ± 0.23 Tmol/year; Tucker et al., 2018). The modern metamorphic decarbonation flux from the active Himalayan orogen and global continental arcs was estimated as ~1.67 Tmol/year (Becker et al., 2008; Ramos et al., 2020). The continental crust could thus currently be a net carbon sink. Alternatively, other decarbonation fluxes of continental crust have yet to be identified, such as the remobilization of continental crustal carbonate caused by intraplate magmatism (Ganino & Arndt, 2009). The preserved crustal rock volumes reconstructed from the Macrostrat stratigraphic database (3.0 Ga–present) show that the global accretion rate of sedimentary rocks has remained approximately constant for the past 500 million years and about 47 times higher than that in Precambrian (Walton et al., 2023). Thus, the average time-integrated carbonate accretion mass of bulk continental crust can be calculated by scaling the modern net carbonate accretion flux to the past 3 billion years, which yields $5.26^{+5.26}_{-3.08} \times 10^{21}$ mol respectively. Based on the preserved carbon content in modern continental crust (4.24 (±1.21) × $10^{21}$ mol; Hirschmann, 2018), the average time-integrated CPE for continental crust was estimated as ~$80^{+20}_{-43}$%. Despite the large uncertainty, this indicates that continental crust must have served as a long-term net sink of surface carbon. On the other hand, remarkable accreted sedimentary carbonates may have been remobilized in the past. In addition, the tectonomagmatic events that can remobilize accreted sedimentary carbonates were usually episodic (e.g., seismic activities, Girault et al., 2018; continental arc volcanics, Cao et al., 2017) or explosive (e.g., large igneous provinces; Ganino & Arndt, 2009), which rendered the thermal decarbonation flux of continental crust could have significantly fluctuated in the Earth's history. In any case, whether as a long-term sink or a "short-term" source, the continental crust has provided an important driving force for regulating the atmospheric $CO_2$ abundances in the past.

## Data Availability Statement

All the analytical results involved in this study are listed in Supporting Information S1, which are deposited on the open-source Figshare Repository and can be accessed through Shi et al. (2024).

**Acknowledgments**
This study was supported by the National Natural Science Foundation of China (Nos. 42288201, 42121002, 42073035, and 41688103), China Postdoctoral Science Foundation (No. 2023M733310), National Key Research and Development Project of China (Nos. 2022YFF0800901, 2023YFF0804304), Second Tibetan Plateau Scientific Expedition and Research (STEP) program (No. 2019QZKK0702), Fundamental Research Funds for the Central Universities (No. 2652023001), and 111 Program (No. B18048). The studied carbonate-bearing samples were collected during several field campaigns in central-eastern Nepal funded by the Italian Ministry of University and Research (Nos. PRIN2006, PRIN2010–2011, PRIN2015, PRIN2017, PRIN2022; 2006040882_003; 2010PMKZX7; 2015EC9PJ5; 2017LMNLAW; 2022HA8XCS). We thank Wenning Lu and Yang Wang for their help on the isotopic analysis and Craig Walton for insightful discussions. We greatly appreciate the handling of Quentin Williams and the constructive comments from Emille Beller and the other anonymous reviewer.

## References

Becker, J. A., Bickle, M. J., Galy, A., & Holland, T. J. B. (2008). Himalayan metamorphic $CO_2$ fluxes: Quantitative constraints from hydrothermal springs. *Earth and Planetary Science Letters*, *265*(3–4), 616–629. https://doi.org/10.1016/j.epsl.2007.10.046

Berner, R. A. (1980). *Early diagenesis: A theoretical approach*. Princeton University Press.

Byrnes, A. P., & Wyllie, P. J. (1981). Subsolidus and melting relations for the join $CaCO_3$-$MgCO_3$ at 10 kbar. *Geochimica et Cosmochimica Acta*, *45*(3), 321–328. https://doi.org/10.1016/0016-7037(81)90242-8

Cao, W., Lee, C.-T. A., & Lackey, J. S. (2017). Episodic nature of continental arc activity since 750 Ma: A global compilation. *Earth and Planetary Science Letters*, *461*, 85–95. https://doi.org/10.1016/j.epsl.2016.12.044

Chanda, P., & Fantle, M. S. (2017). Quantifying the effect of diagenetic recrystallization on the Mg isotopic composition of marine carbonates. *Geochimica et Cosmochimica Acta*, *204*, 219–239. https://doi.org/10.1016/j.gca.2017.01.010

DePaolo, D. J. (2015). Sustainable carbon emissions: The geologic perspective. *MRS Energy & Sustainability*, *2*, 1–16. https://doi.org/10.1557/mre.2015.10

Fantle, M. S., Barnes, B. D., & Lau, K. V. (2020). The role of diagenesis in shaping the geochemistry of the marine carbonate record. *Annual Review of Earth and Planetary Sciences*, *48*(1), 549–583. https://doi.org/10.1146/annurev-earth-073019-060021

Ferrero, S., Wunder, B., Ziemann, M. A., Wälle, M., & O'Brien, P. J. (2016). Carbonatitic and granitic melts produced under conditions of primary immiscibility during anatexis in the lower crust. *Earth and Planetary Science Letters*, *454*, 121–131. https://doi.org/10.1016/j.epsl.2016.08.043

Ganino, C., & Arndt, N. T. (2009). Climate changes caused by degassing of sediments during the emplacement of large igneous provinces. *Geology*, *37*(4), 323–326. https://doi.org/10.1130/g25325a.1

Gao, S., Luo, T.-C., Zhang, B.-R., Zhang, H.-F., Han, Y.-W., Zhao, Z.-D., & Hu, Y.-K. (1998). Chemical composition of the continental crust as revealed by studies in East China. *Geochimica et Cosmochimica Acta*, *62*(11), 1959–1975. https://doi.org/10.1016/S0016-7037(98)00121-5

Geske, A., Goldstein, R. H., Mavromatis, V., Richter, D. K., Buhl, D., Kluge, T., et al. (2015). The magnesium isotope ($\delta^{26}$Mg) signature of dolomites. *Geochimica et Cosmochimica Acta*, *149*, 131–151. https://doi.org/10.1016/j.gca.2014.11.003

Girault, F., Adhikari, L. B., France-Lanord, C., Agrinier, P., Koirala, B. P., Bhattarai, M., et al. (2018). Persistent $CO_2$ emissions and hydrothermal unrest following the 2015 earthquake in Nepal. *Nature Communications*, *9*(1), 2956. https://doi.org/10.1038/s41467-018-05138-z

Groppo, C., Rapa, G., Frezzotti, M. L., & Rolfo, F. (2021). The fate of calcareous pelites in collisional orogens. *Journal of Metamorphic Geology*, *39*(2), 181–207. https://doi.org/10.1111/jmg.12568

Groppo, C., Rolfo, F., Castelli, D., & Mosca, P. (2017). Metamorphic $CO_2$ production in collisional orogens: Petrological constraints from phase diagram modeling of Himalayan, Scapolite-bearing, Calc-silicate rocks in the NKC(F)MAS(T)-HC system. *Journal of Petrology*, *58*(1), 53–83. https://doi.org/10.1093/petrology/egx005

Groppo, C., Rolfo, F., & Frezzotti, M. L. (2022). $CO_2$ outgassing during collisional orogeny is facilitated by the generation of immiscible fluids. *Communications Earth & Environment*, *3*(1), 13. https://doi.org/10.1038/s43247-022-00340-w

Higgins, J. A., Blättler, C. L., Lundstrom, E. A., Santiago-Ramos, D. P., Akhtar, A. A., Crüger Ahm, A. S., et al. (2018). Mineralogy, early marine diagenesis, and the chemistry of shallow-water carbonate sediments. *Geochimica et Cosmochimica Acta*, *220*, 512–534. https://doi.org/10.1016/j.gca.2017.09.046

Hirschmann, M. M. (2018). Comparative deep Earth volatile cycles: The case for C recycling from exosphere/mantle fractionation of major ($H_2O$, C, N) volatiles and from $H_2O$/Ce, $CO_2$/Ba, and $CO_2$/Nb exosphere ratios. *Earth and Planetary Science Letters*, *502*, 262–273. https://doi.org/10.1016/j.epsl.2018.08.023

Hu, Y., Teng, F.-Z., Plank, T., & Huang, K.-J. (2017). Magnesium isotopic composition of subducting marine sediments. *Chemical Geology*, *466*, 15–31. https://doi.org/10.1016/j.chemgeo.2017.06.010

Hunt, J. M. (1972). Distribution of carbon in crust of Earth. *AAPG Bulletin*, *56*(11), 2273–2277. https://doi.org/10.1306/819A4206-16C5-11D7-8645000102C1865D

Lee, C.-T. A., Jiang, H., Dasgupta, R., & Torres, M. (2019). A framework for understanding whole-Earth carbon cycling. In B. N. Orcutt, I. Daniel, & R. Dasgupta (Eds.), *Deep carbon: Past to present* (pp. 313–357). Cambridge University Press.

Li, W.-Y., Teng, F.-Z., Ke, S., Rudnick, R. L., Gao, S., Wu, F.-Y., & Chappell, B. W. (2010). Heterogeneous magnesium isotopic composition of the upper continental crust. *Geochimica et Cosmochimica Acta*, *74*(23), 6867–6884. https://doi.org/10.1016/j.gca.2010.08.030

Liu, S.-A., Teng, F.-Z., He, Y., Ke, S., & Li, S. (2010). Investigation of magnesium isotope fractionation during granite differentiation: Implication for Mg isotopic composition of the continental crust. *Earth and Planetary Science Letters*, *297*(3–4), 646–654. https://doi.org/10.1016/j.epsl.2010.07.019

Mason, E., Edmonds, M., & Turchyn, A. V. (2017). Remobilization of crustal carbon may dominate volcanic arc emissions. *Science*, *357*(6348), 4–294. https://doi.org/10.1126/science.aan5049

Qu, Y.-R., Liu, S.-A., Wu, H., Li, M.-L., & Tian, H.-C. (2022). Tracing carbonate dissolution in subducting sediments by zinc and magnesium isotopes. *Geochimica et Cosmochimica Acta*, *319*, 56–72. https://doi.org/10.1016/j.gca.2021.12.020

Ramos, E., Lackey, J. S., Barnes, J., & Fulton, A. (2020). Remnants and rates of metamorphic decarbonation in continental arcs. *Geological Society of America Today*, *30*(5), 4–10. https://doi.org/10.1130/gsatg432a.1

Rapa, G., Groppo, C., Rolfo, F., Petrelli, M., Mosca, P., & Perugini, D. (2017). Titanite-bearing calc-silicate rocks constrain timing, duration and magnitude of metamorphic $CO_2$ degassing in the Himalayan belt. *Lithos*, *292–293*, 364–378. https://doi.org/10.1016/j.lithos.2017.09.024

Rolfo, F., Groppo, C., & Mosca, P. (2017). Metamorphic $CO_2$ production in calc-silicate rocks from the eastern Himalaya. *Italian Journal of Geosciences*, *136*(1), 28–33. https://doi.org/10.3301/ijg.2015.36

Ronov, A., Yaroshevskiy, A., & Migdisov, A. (1991). Chemical constitution of the Earth's crust and geochemical balance of the major elements. *International Geology Review*, *33*(10), 941–1048. https://doi.org/10.1080/00206819109465736

Shi, Q., He, Y., Zhao, Z., Liu, D., Harris, N., & Zhu, D. C. (2021). Petrogenesis of Himalayan leucogranites: Perspective from a combined elemental and Fe-Sr-Nd isotope study. *Journal of Geophysical Research: Solid Earth*, *126*(8), e2021JB021839. https://doi.org/10.1029/2021JB021839

Shi, Q., He, Y., Zhao, Z., Rolfo, F., Groppo, C., Harris, N. B. W., et al. (2024). Supporting information for "Magnesium isotopes archive the initial carbonate abundances of metasedimentary rocks prior to thermal decarbonation" (Version 2) [Dataset]. *Figshare*. https://doi.org/10.6084/m9.figshare.24319837.v2

Stewart, E. M., Ague, J. J., Ferry, J. M., Schiffries, C. M., Tao, R.-B., Isson, T. T., & Planavsky, N. J. (2019). Carbonation and decarbonation reactions: Implications for planetary habitability. *American Mineralogist*, *104*(10), 1369–1380. https://doi.org/10.2138/am-2019-6884

Tacchetto, T., Bartoli, O., Cesare, B., Berkesi, M., Aradi, L. E., Dumond, G., & Szabó, C. (2019). Multiphase inclusions in peritectic garnet from granulites of the Athabasca granulite terrane (Canada): Evidence of carbon recycling during Neoarchean crustal melting. *Chemical Geology*, *508*, 197–209. https://doi.org/10.1016/j.chemgeo.2018.05.043

Teng, F.-Z. (2017). Magnesium isotope geochemistry. *Reviews in Mineralogy and Geochemistry*, *82*(1), 219–287. https://doi.org/10.2138/rmg.2017.82.7

Tucker, J. M., Mukhopadhyay, S., & Gonnermann, H. M. (2018). Reconstructing mantle carbon and noble gas contents from degassed mid-ocean ridge basalts. *Earth and Planetary Science Letters*, *496*, 108–119. https://doi.org/10.1016/j.epsl.2018.05.024

Walton, C. R., Hao, J., Huang, F., Jenner, F. E., Williams, H., Zerkle, A. L., et al. (2023). Evolution of the crustal phosphorus reservoir. *Science Advances*, *9*(18), eade6923. https://doi.org/10.1126/sciadv.ade6923

Wang, S. J., Teng, F. Z., & Li, S. G. (2014). Tracing carbonate-silicate interaction during subduction using magnesium and oxygen isotopes. *Nature Communications*, *5*(1), 5328. https://doi.org/10.1038/ncomms6328

Wang, S.-J., Teng, F.-Z., Rudnick, R. L., & Li, S.-G. (2015). The behavior of magnesium isotopes in low-grade metamorphosed mudrocks. *Geochimica et Cosmochimica Acta*, *165*, 435–448. https://doi.org/10.1016/j.gca.2015.06.019

Yang, W., Teng, F.-Z., Li, W.-Y., Liu, S.-A., Ke, S., Liu, Y.-S., et al. (2016). Magnesium isotopic composition of the deep continental crust. *American Mineralogist*, *101*(2), 243–252. https://doi.org/10.2138/am-2016-5275

Zhu, R., Zhao, G., Xiao, W., Chen, L., & Tang, Y. (2021). Origin, accretion, and reworking of continents. *Reviews of Geophysics*, *59*(3), e2019RG000689. https://doi.org/10.1029/2019rg000689

## References From the Supporting Information

Ahm, A.-S. C., Bjerrum, C. J., Hoffman, P. F., Macdonald, F. A., Maloof, A. C., Rose, C. V., et al. (2021). The Ca and Mg isotope record of the Cryogenian Trezona carbon isotope excursion. *Earth and Planetary Science Letters*, *568*, 117002. https://doi.org/10.1016/j.epsl.2021.117002

An, Y., Wu, F., Xiang, Y., Nan, X., Yu, X., Yang, J., et al. (2014). High-precision Mg isotope analyses of low-Mg rocks by MC-ICP-MS. *Chemical Geology*, *390*, 9–21. https://doi.org/10.1016/j.chemgeo.2014.09.014

Azmy, K., Lavoie, D., Wang, Z., Brand, U., Al-Aasm, I., Jackson, S., & Girard, I. (2013). Magnesium-isotope and REE compositions of Lower Ordovician carbonates from eastern Laurentia: Implications for the origin of dolomites and limestones. *Chemical Geology*, *356*, 64–75. https://doi.org/10.1016/j.chemgeo.2013.07.015

Bialik, O. M., Wang, X., Zhao, S., Waldmann, N. D., Frank, R., & Li, W. (2018). Mg isotope response to dolomitization in hinterland-attached carbonate platforms: Outlook of $\delta^{26}$Mg as a tracer of basin restriction and seawater Mg/Ca ratio. *Geochimica et Cosmochimica Acta*, *235*, 189–207. https://doi.org/10.1016/j.gca.2018.05.024

Blättler, C. L., Miller, N. R., & Higgins, J. A. (2015). Mg and Ca isotope signatures of authigenic dolomite in siliceous deep-sea sediments. *Earth and Planetary Science Letters*, *419*, 32–42. https://doi.org/10.1016/j.epsl.2015.03.006

Bold, U., Ahm, A.-S. C., Schrag, D. P., Higgins, J. A., Jamsran, E., & Macdonald, F. A. (2020). Effect of dolomitization on isotopic records from Neoproterozoic carbonates in southwestern Mongolia. *Precambrian Research*, *350*, 105902. https://doi.org/10.1016/j.precamres.2020.105902

Brenot, A., Cloquet, C., Vigier, N., Carignan, J., & France-Lanord, C. (2008). Magnesium isotope systematics of the lithologically varied Moselle river basin, France. *Geochimica et Cosmochimica Acta*, *72*(20), 5070–5089. https://doi.org/10.1016/j.gca.2008.07.027

Buhl, D., Immenhauser, A., Smeulders, G., Kabiri, L., & Richter, D. K. (2007). Time series $\delta^{26}$Mg analysis in speleothem calcite: Kinetic versus equilibrium fractionation, comparison with other proxies and implications for palaeoclimate research. *Chemical Geology*, *244*(3–4), 715–729. https://doi.org/10.1016/j.chemgeo.2007.07.019

Caciagli, N. C., & Manning, C. E. (2003). The solubility of calcite in water at 6-16 kbar and 500-800°C. *Contributions to Mineralogy and Petrology*, *146*(3), 275–285. https://doi.org/10.1007/s00410-003-0501-y

Crockford, P. W., Kunzmann, M., Blättler, C. L., Kalderon-Asael, B., Murphy, J. G., Ahm, A.-S., et al. (2020). Reconstructing Neoproterozoic seawater chemistry from early diagenetic dolomite. *Geology*, *49*(4), 442–446. https://doi.org/10.1130/g48213.1

Fantle, M. S., & Higgins, J. (2014). The effects of diagenesis and dolomitization on Ca and Mg isotopes in marine platform carbonates: Implications for the geochemical cycles of Ca and Mg. *Geochimica et Cosmochimica Acta*, *142*, 458–481. https://doi.org/10.1016/j.gca.2014.07.025

Gaillardet, J., Dupré, B., Louvat, P., & Allegre, C. (1999). Global silicate weathering and $CO_2$ consumption rates deduced from the chemistry of large rivers. *Chemical Geology*, *159*(1–4), 3–30. https://doi.org/10.1016/s0009-2541(99)00031-5

Galy, A., Bar-Matthews, M., Halicz, L., & O'Nions, R. K. (2002). Mg isotopic composition of carbonate: Insight from speleothem formation. *Earth and Planetary Science Letters*, *201*(1), 105–115. https://doi.org/10.1016/S0012-821X(02)00675-1

Gao, T., Ke, S., Li, R., Meng, X., He, Y., Liu, C., et al. (2019). High-precision magnesium isotope analysis of geological and environmental reference materials by multiple-collector inductively coupled plasma mass spectrometry. *Rapid Communications in Mass Spectrometry*, *33*(8), 767–777. https://doi.org/10.1002/rcm.8376

Geske, A., Zorlu, J., Richter, D. K., Buhl, D., Niedermayr, A., & Immenhauser, A. (2012). Impact of diagenesis and low grade metamorphosis on isotope ($\delta^{26}$Mg, $\delta^{13}$C, $\delta^{18}$O, and $^{87}$Sr/$^{86}$Sr) and elemental (Ca, Mg, Mn, Fe, and Sr) signatures of Triassic sabkha dolomites. *Chemical Geology*, *332–333*, 45–64. https://doi.org/10.1016/j.chemgeo.2012.09.014

He, R., Ning, M., Huang, K., Ma, H., & Shen, B. (2020). Mg isotopic systematics during early diagenetic aragonite-calcite transition: Insights from the Key Largo Limestone. *Chemical Geology*, *558*, 119876. https://doi.org/10.1016/j.chemgeo.2020.119876

He, Y., Sun, A.-Y., Zhang, Y.-C., Yang, R.-Y., Ke, S., Wang, Y., & Teng, F.-Z. (2022). High-precision and high-accuracy magnesium isotope analysis on multiple-collector inductively coupled plasma mass spectrometry using a critical mixture double spike technique. *Solid Earth Sciences*, *7*(3), 188–199. https://doi.org/10.1016/j.sesci.2022.05.001

Higgins, J. A., & Schrag, D. P. (2012). Records of Neogene seawater chemistry and diagenesis in deep-sea carbonate sediments and pore fluids. *Earth and Planetary Science Letters*, *357–358*, 386–396. https://doi.org/10.1016/j.epsl.2012.08.030

Higgins, J. A., & Schrag, D. P. (2015). The Mg isotopic composition of Cenozoic seawater—Evidence for a link between Mg-clays, seawater Mg/Ca, and climate. *Earth and Planetary Science Letters*, *416*, 73–81. https://doi.org/10.1016/j.epsl.2015.01.003

Holland, H. D. (2005). Sea level, sediments and the composition of seawater. *American Journal of Science*, *305*(3), 220–239. https://doi.org/10.2475/ajs.305.3.220

Huang, H., Niu, Y., Teng, F.-Z., & Wang, S.-J. (2019). Discrepancy between bulk-rock and zircon Hf isotopes accompanying Nd-Hf isotope decoupling. *Geochimica et Cosmochimica Acta*, *259*, 17–36. https://doi.org/10.1016/j.gca.2019.05.031

Huang, K.-J., Shen, B., Lang, X.-G., Tang, W.-B., Peng, Y., Ke, S., et al. (2015). Magnesium isotopic compositions of the Mesoproterozoic dolostones: Implications for Mg isotopic systematics of marine carbonates. *Geochimica et Cosmochimica Acta*, *164*, 333–351. https://doi.org/10.1016/j.gca.2015.05.002

Hu, Z., Bialik, O. M., Hohl, S. V., Xia, Z., Waldmann, N. D., Liu, C., & Li, W. (2021a). Response of Mg isotopes to dolomitization during fluctuations in sea level: Constraints on the hydrological conditions of massive dolomitization systems. *Sedimentary Geology*, *420*, 105922. https://doi.org/10.1016/j.sedgeo.2021.105922

Hu, Z., Li, W., Zhang, H., Krainer, K., Zheng, Q.-F., Xia, Z., et al. (2021b). Mg isotope evidence for restriction events within the Paleotethys ocean around the Permian-Triassic transition. *Earth and Planetary Science Letters*, *556*, 116704. https://doi.org/10.1016/j.epsl.2020.116704

Hu, Z., Shi, Z., Li, G., Xia, Z., Yi, L., Liu, C., & Li, W. (2022). The Cenozoic Seawater Conundrum: New constraints from Mg isotopes in island dolostones. *Earth and Planetary Science Letters*, *595*, 117755. https://doi.org/10.1016/j.epsl.2022.117755

Immenhauser, A., Buhl, D., Richter, D., Niedermayr, A., Riechelmann, D., Dietzel, M., & Schulte, U. (2010). Magnesium-isotope fractionation during low-Mg calcite precipitation in a limestone cave—Field study and experiments. *Geochimica et Cosmochimica Acta*, *74*(15), 4346–4364. https://doi.org/10.1016/j.gca.2010.05.006

Jacobson, A. D., Zhang, Z., Lundstrom, C., & Huang, F. (2010). Behavior of Mg isotopes during dedolomitization in the Madison Aquifer, South Dakota. *Earth and Planetary Science Letters*, *297*(3–4), 446–452. https://doi.org/10.1016/j.epsl.2010.06.038

Kasemann, S. A., Pogge von Strandmann, P. A. E., Prave, A. R., Fallick, A. E., Elliott, T., & Hoffmann, K.-H. (2014). Continental weathering following a Cryogenian glaciation: Evidence from calcium and magnesium isotopes. *Earth and Planetary Science Letters*, *396*, 66–77. https://doi.org/10.1016/j.epsl.2014.03.048

Ke, S., Teng, F.-Z., Li, S.-G., Gao, T., Liu, S.-A., He, Y., & Mo, X. (2016). Mg, Sr, and O isotope geochemistry of syenites from northwest Xinjiang, China: Tracing carbonate recycling during Tethyan oceanic subduction. *Chemical Geology*, *437*, 109–119. https://doi.org/10.1016/j.chemgeo.2016.05.002

Lan, C., Tao, R., Huang, F., Jiang, R., & Zhang, L. (2023). High-pressure experimental and thermodynamic constraints on the solubility of carbonates in subduction zone fluids. *Earth and Planetary Science Letters*, *603*, 117989. https://doi.org/10.1016/j.epsl.2023.117989

Lee, S.-G., Ahn, I., Asahara, Y., Tanaka, T., & Lee, S. R. (2018). Geochemical interpretation of magnesium and oxygen isotope systematics in granites with the REE tetrad effect. *Geosciences Journal*, *22*(5), 697–710. https://doi.org/10.1007/s12303-018-0024-1

Li, R.-Y., Ke, S., Li, S., Song, S., Wang, C., & Liu, C. (2020). Origins of two types of Archean potassic granite constrained by Mg isotopes and statistical geochemistry: Implications for continental crustal evolution. *Lithos*, *368–369*, 105570. https://doi.org/10.1016/j.lithos.2020.105570

Li, S., Miller, C. F., Tao, W., Xiao, W., & Chew, D. (2021). Role of sediment in generating contemporaneous, diverse "type" granitoid magmas. *Geology*, *50*(4), 427–431. https://doi.org/10.1130/g49509.1

Li, W., Bialik, O. M., Wang, X., Yang, T., Hu, Z., Huang, Q., et al. (2019). Effects of early diagenesis on Mg isotopes in dolomite: The roles of Mn (IV)-reduction and recrystallization. *Geochimica et Cosmochimica Acta*, *250*, 1–17. https://doi.org/10.1016/j.gca.2019.01.029

Li, W.-Y., Teng, F.-Z., Wing, B. A., & Xiao, Y. (2014). Limited magnesium isotope fractionation during metamorphic dehydration in metapelites from the Onawa contact aureole, Maine. *Geochemistry, Geophysics, Geosystems*, *15*(2), 408–415. https://doi.org/10.1002/2013gc004992

Liu, C., Wang, Z., Raub, T. D., Macdonald, F. A., & Evans, D. A. D. (2014). Neoproterozoic cap-dolostone deposition in stratified glacial meltwater plume. *Earth and Planetary Science Letters*, *404*, 22–32. https://doi.org/10.1016/j.epsl.2014.06.039

Ma, H., Xu, Y., Huang, K., Sun, Y., Ke, S., Peng, Y., et al. (2018). Heterogeneous Mg isotopic composition of the early Carboniferous limestone: Implications for carbonate as a seawater archive. *Acta Geochimica*, *37*(1), 1–18. https://doi.org/10.1007/s11631-017-0179-x

Nelson, L. L., Ahm, A.-S. C., Macdonald, F. A., Higgins, J. A., & Smith, E. F. (2021). Fingerprinting local controls on the Neoproterozoic carbon cycle with the isotopic record of Cryogenian carbonates in the Panamint Range, California. *Earth and Planetary Science Letters*, *566*, 116956. https://doi.org/10.1016/j.epsl.2021.116956

Ning, M., Huang, K., Lang, X., Ma, H., Yuan, H., Peng, Y., & Shen, B. (2019). Can crystal morphology indicate different generations of dolomites? Evidence from magnesium isotopes. *Chemical Geology*, *516*, 1–17. https://doi.org/10.1016/j.chemgeo.2019.04.007

Ning, M., Lang, X., Huang, K., Li, C., Huang, T., Yuan, H., et al. (2020). Towards understanding the origin of massive dolostones. *Earth and Planetary Science Letters*, *545*, 116403. https://doi.org/10.1016/j.epsl.2020.116403

Patiño Douce, A. E., & Harris, N. (1998). Experimental constraints on Himalayan anatexis. *Journal of Petrology*, *39*(4), 689–710. https://doi.org/10.1093/petroj/39.4.689

Pokrovsky, B. G., Mavromatis, V., & Pokrovsky, O. S. (2011). Co-variation of Mg and C isotopes in late Precambrian carbonates of the Siberian Platform: A new tool for tracing the change in weathering regime? *Chemical Geology*, *290*(1–2), 67–74. https://doi.org/10.1016/j.chemgeo.2011.08.015

Rapa, G., Mosca, P., Groppo, C., & Rolfo, F. (2018). Detection of tectonometamorphic discontinuities within the Himalayan orogen: Structural and petrological constraints from the Rasuwa district, central Nepal Himalaya. *Journal of Asian Earth Sciences*, *158*, 266–286. https://doi.org/10.1016/j.jseaes.2018.02.021

Shalev, N., Bontognali, T. R. R., Wheat, C. G., & Vance, D. (2019). New isotope constraints on the Mg oceanic budget point to cryptic modern dolomite formation. *Nature Communications*, *10*(1), 5646. https://doi.org/10.1038/s41467-019-13514-6

Shen, B., Jacobsen, B., Lee, C.-T. A., Yin, Q.-Z., & Morton, D. M. (2009). The Mg isotopic systematics of granitoids in continental arcs and implications for the role of chemical weathering in crust formation. *Proceedings of the National Academy of Sciences of the United States of America*, *106*(49), 20652–20657. https://doi.org/10.1073/pnas.0910663106

Spencer, C. J., Roberts, N. M. W., & Santosh, M. (2017). Growth, destruction, and preservation of Earth's continental crust. *Earth-Science Reviews*, *172*, 87–106. https://doi.org/10.1016/j.earscirev.2017.07.013

Tamang, S., Groppo, C., Girault, F., & Rolfo, F. (2023). Implications of garnet nucleation overstepping for the P–T evolution of the Lesser Himalayan Sequence of central Nepal. *Journal of Metamorphic Geology*, *41*(2), 271–297. https://doi.org/10.1111/jmg.12695

Telus, M., Dauphas, N., Moynier, F., Tissot, F. L. H., Teng, F.-Z., Nabelek, P. I., et al. (2012). Iron, zinc, magnesium and uranium isotopic fractionation during continental crust differentiation: The tale from migmatites, granitoids, and pegmatites. *Geochimica et Cosmochimica Acta*, *97*, 247–265. https://doi.org/10.1016/j.gca.2012.08.024

Teng, F. Z., Hu, Y., & Chauvel, C. (2016). Magnesium isotope geochemistry in arc volcanism. *Proceedings of the National Academy of Sciences of the United States of America*, *113*(26), 7082–7087. https://doi.org/10.1073/pnas.1518456113

Tian, H.-C., Yang, W., Li, S.-G., Wei, H.-Q., Yao, Z.-S., & Ke, S. (2019). Approach to trace hidden paleo-weathering of basaltic crust through decoupled Mg-Sr and Nd isotopes recorded in volcanic rocks. *Chemical Geology*, *509*, 234–248. https://doi.org/10.1016/j.chemgeo.2019.01.019

Tian, S., Hou, Z., Chen, X., Tian, H., Gong, Y., Yang, Z., et al. (2020). Magnesium isotopic behaviors between metamorphic rocks and their associated leucogranites, and implications for Himalayan orogenesis. *Gondwana Research*, *87*, 23–40. https://doi.org/10.1016/j.gr.2020.06.006

Tipper, E., Galy, A., & Bickle, M. (2006a). Riverine evidence for a fractionated reservoir of Ca and Mg on the continents: Implications for the oceanic Ca cycle. *Earth and Planetary Science Letters*, *247*(3–4), 267–279. https://doi.org/10.1016/j.epsl.2006.04.033

Tipper, E., Galy, A., Gaillardet, J., Bickle, M., Elderfield, H., & Carder, E. (2006b). The magnesium isotope budget of the modern ocean: Constraints from riverine magnesium isotope ratios. *Earth and Planetary Science Letters*, *250*(1–2), 241–253. https://doi.org/10.1016/j.epsl.2006.07.037

Wang, Y., He, Y., & Ke, S. (2020a). Mg isotope fractionation during partial melting of garnet-bearing sources: An adakite perspective. *Chemical Geology*, *537*, 119478. https://doi.org/10.1016/j.chemgeo.2020.119478

Wang, Z.-Z., Liu, S.-A., Liu, Z.-C., Zheng, Y.-C., & Wu, F.-Y. (2020b). Extreme Mg and Zn isotope fractionation recorded in the Himalayan leucogranites. *Geochimica et Cosmochimica Acta*, *278*, 305–321. https://doi.org/10.1016/j.gca.2019.09.026

Wilkinson, B. H., & Algeo, T. J. (1989). Sedimentary carbonate record of calcium-magnesium cycling. *American Journal of Science*, *289*(10), 1158–1194. https://doi.org/10.2475/ajs.289.10.1158

Xing, C., Ning, M., Huang, T., Huang, K., Li, C., Zhao, Z., et al. (2021). Testing micrite as an ancient seawater Mg isotopic composition archive: A case study of Upper Paleozoic carbonate. *Palaeogeography, Palaeoclimatology, Palaeoecology*, *567*, 110278. https://doi.org/10.1016/j.palaeo.2021.110278

Zeng, S., Liu, Z., & Groves, C. (2022). Large-scale $CO_2$ removal by enhanced carbonate weathering from changes in land-use practices. *Earth-Science Reviews*, *225*, 103915. https://doi.org/10.1016/j.earscirev.2021.103915

Zhang, P., Huang, K.-J., Luo, M., Cai, Y., & Bao, Z. (2022). Constraining the terminal Ediacaran seawater chemistry by Mg isotopes in dolostones from the Yangtze Platform, South China. *Precambrian Research*, *377*, 106700. https://doi.org/10.1016/j.precamres.2022.106700

Zou, L., Dong, L., Ning, M., Huang, K., Peng, Y., Qin, S., et al. (2019). Quantifying the carbon source of pedogenic calcite veins in weathered limestone: Implications for the terrestrial carbon cycle. *Acta Geochimica*, *38*(4), 481–496. https://doi.org/10.1007/s11631-019-00348-8